RSC Advances

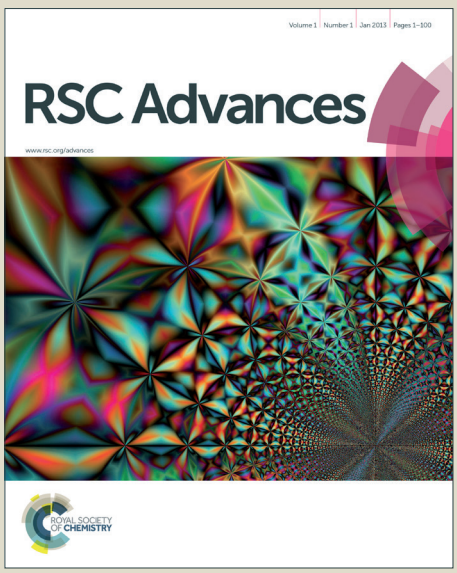

ROYAL SOCIETY OF CHEMISTRY

www.rsc.org/advances

Novel Synthesis of $LiMnPO_4 \cdot Li_3V_2(PO_4)_3$/C Composite Cathode Material

Bao Zhang, Xiao-wei Wang, Jia-feng Zhang[*]

School of Metallurgy and Environment, Central South University, Changsha, 410083, PR China

Abstract: Carbon-coated $LiMnPO_4 \cdot Li_3V_2(PO_4)_3$ composite cathode material is synthesized from rod-like $MnV_2O_6 \cdot 4H_2O$ precursor prepared via aqueous precipitation for the first time, following chemical reduction and lithiation with oxalic acid as the reducing agent and glucose as the carbon source. The XRD results indicate orthorhombic $LiMnPO_4$ and monoclinic $Li_3V_2(PO_4)_3$ are co-existed. The SEM results reveal that the thickness of rod-like $MnV_2O_6 \cdot 4H_2O$ precursor is about 80nm and the $LiMnPO_4 \cdot Li_3V_2(PO_4)_3$/C composite possess a micro-nano spherical-like morphology. HRTEM results indicate the sample is a core-shell structure, which the external shell is amorphous carbon and the core of the sample are $LiMnPO_4$, $Li_3V_2(PO_4)_3$ and $LiMnPO_4 \cdot Li_3V_2(PO_4)_3$ unit cell. The initial discharge capacity of $LiMnPO_4 \cdot Li_3V_2(PO_4)_3$/C composite delivers 110 mAh g^{-1}, 104.4 mAh g^{-1}, 100.6 mAh g^{-1} and 80.4 mAh g^{-1} at the rate of 0.1C, 1C, 3C and 10C, respectively. The cell shows the excellent cycling stability and good rate capability as a cathode for lithium-ion batteries.

Keywords: Lithium ion battery, Cathode material, $MnV_2O_6 \cdot 4H_2O$, $LiMnPO_4 \cdot Li_3V_2(PO_4)_3$/C

Introduction

Rechargable lithium-ion batteries have been the excellent candidates with its high energy density, long cycle life and environmental friendliness since the the increasing environmental pressure. Multiply kinds of materials for cathode and anodes have been invented with the effort of scientists around the world. Among them, metal polyanion material based on phosphate compounds, such as $LiFePO_4$[1], $LiMnPO_4$[2,3], $LiCoPO_4$, $Li_3V_2(PO_4)_3$ [4-7], have been proposed to played an important part in the hybrid electric vehicles, electric vehicles (EVs) and large-scale energy storage, due to their high energy density and durable cycle life. Moreover, the strong P-O bond and three-dimensional solid framework in $(PO_4)^{3-}$ anions can guarantee both the dynamic

*Corresponding author: Jia-feng Zhang is with the School of Metallurgy and Environment, Central South University, PR China. (Phone: +86 731-88836357; Email: csuzjf@vip.163.com).

and thermal stability required to fulfill the safety in high power application mentioned above.

Compared to the commercially successful $LiFePO_4$, $LiMnPO_4$ has an equal theoretical capacity (171mAh g^{-1}), but can provide nearly 20% higher energy density. However, the low electronic conductivity of $LiMnPO_4$ limit its performance at high currents[8]. Corresponding to $LiMnPO_4$, $Li_3V_2(PO_4)_3$ has been proposed to be a highly promising cathode material for high-power lithium ion batteries because of its open three-dimensional framework, which allows fast transport of lithium ion[9]. Many efforts including metal-doping[10-13], coating with the electronically conductive materials like carbon, metal, and metal oxide[14,15-17], and optimization of particles with suitable preparation procedures have been made to improve the performance of $LiMnPO_4$ and $Li_3V_2(PO_4)_3$ cathode materials. Recently, Yang et al[18] reported that the discharge capacity at 1/20C in the voltage range of 2.7-4.8 V was 10 mAh g^{-1} for $LiMn_{0.95}V_{0.05}PO_4$ and 62 mAh g^{-1} for pure $LiMnPO_4$. Wang et al[19] reported the performance of different ratio of $LiMnPO_4$ and $Li_2V_2(PO_4)_3$ in the composite synthesized through a spray drying followed by solid-state reaction and reported the electronic conductivity of the $LiMnPO_4$ could be enhanced by adding some $Li_3V_2(PO_4)_3$. Qin et al[20] reported the relationship between the ratios of $LiMnPO_4$ to $Li_3V_2(PO_4)_3$ and the electrochemical performances of the composite materials, indicating the best ratio of 0.6:0.4.

In this work, we reported a new way to synthesize $LiMnPO_4 \cdot Li_3V_2(PO_4)_3$/C composite cathode material. We used NH_4VO_3 and $Mn(CH_3COO) \cdot 4H_2O$ as starting materials to synthesize rod-like $MnV_2O_6 \cdot 4H_2O$ precursor via aqueous co-precipitation route for the first time and $LiMnPO_4 \cdot Li_3V_2(PO_4)_3$/C was prepared from the $MnV_2O_6 \cdot 4H_2O$ precursor by chemical reduction, and the properties were innovationally investigated .

Experimental section

Rod-like $MnV_2O_6 \cdot 4H_2O$ particles was synthesized via aqueous co-precipitation route for the first time. An equimolar solution of $Mn(CH_3COO)_2 \cdot 4H_2O$ (99 wt.%) and NH_4VO_3 (99 wt.%) were mixed under vigorous stirring and maintained at 60°C for 1 h under ultrasonic dispersion. The pH value of the solution was employed to be adjusted to 6 by using ammonia water. Then a brick-red precipitate spontaneously appeared and remained. $MnV_2O_6 \cdot 4H_2O$ precursor was washed for three times with deionized water and dried in an oven at 60°C. Then the stoichiometric ratio of

$MnV_2O_6 \cdot 4H_2O$ precursor, LiH_2PO_4 (99.9 wt.%), oxalic acid, and glucose were mixed by ball milling for 4 h in alcohol, the oxalic acid is the reducer and the glucose works as carbon source. The resulting mixture was dried at 60°C and subsequently fired in argon atmosphere. Finally the $LiMnPO_4 \cdot Li_3V_2(PO_4)_3$/C was obtained. The reaction may occur as the follows,

$$MnV_2O_6 \cdot 4H_2O + 4LiH_2PO_4 + 4HOOCCOOH \cdot 2H_2O \rightarrow LiMnPO_4 + Li_3V_2(PO_4)_3 + 8CO_2\uparrow + 12H_2O\uparrow \quad (1)$$

The mole ratio Mn/V of as-prepared $MnV_2O_6 \cdot 4H_2O$ was determined by chemical titration. Furthermore, the powder X-ray diffraction (Rint-2000, Rigaku) measurement using Cu Kradiation was employed to identify the crystalline structure and purity of the synthesized materials. The surface morphologies and particle information of samples were observed by SEM (JEOL, JSM-5600LV) and transmission electron microscope(TEM) (Tecnai G12). Analysis on carbon content of the composite was performed by C-S analysis equipment (Eltar, Germany).

The electrochemical characterization were detected using CR2025 coin-type cell. Typical positive electrode loadings were in the range of 2-2.5 mg cm^{-2}, and an electrode diameter of 14 mm was used. For positive electrode fabrication, the prepared powders were mixed with 10% of carbon black and 10% of polyvinylidene fluoride in N-methyl pyrrolidinone until slurry was obtained. And then, the blended slurries were pasted onto an aluminum current collector, and the electrode was dried at 120°C for 4 h in the air. The test cell consisted of the positive electrode and lithium foil negative electrode separated by a porous polypropylene film, and 1 mol L^{-1} $LiPF_6$ in EC, EMC and DMC (1:1:1 in volume) as the electrolyte. In addition, the assembly of the cells was carried out in a dry Ar-filled glove box. The coin cells were charged at 0.1C rate and discharged at the rates of 0.1C, 1C, 5C and 10C over the voltage range of 2.5-4.5V at ambient temperature using a battery testing system (Neware BTS-2000). Finally, cyclic voltammogram was carried out with a CHI660D electrochemical analyzer.

Results

Rod-like $MnV_2O_6 \cdot 4H_2O$ precursor was innovationally prepared via aqueous co-precipitation process. Based on analysis of chemical titration, the Mn/V mole ratio of $MnV_2O_6 \cdot xH_2O$ is 2.003, confirming that the prepared brick-red precipitate is $MnV_2O_6 \cdot xH_2O$.

Fig.1 shows the XRD patterns of $MnV_2O_6 \cdot 4H_2O$. All the peaks are indexed and consistent with the data of JCPDS#86-0720. The crystal structure is identified to be monoclinic structure, the

same as that reported by JOEL [23].

As illustrated in Fig.2, the main part of the obtained $MnV_2O_6 \cdot 4H_2O$ are rod-like, with the average width of the particle around 200nm and the thickness approaching 100nm. A small number of rods aggregate and make rods with the width and thickness approaching 2μm.

Fig.3 shows the typical Rietveld refinement XRD patterns of LMP·LVP/C synthesized at 700°C for 10 h. The refined lattice parameters and phase content are listed in Table.1. The observed and calculated patterns match well, and the reliability factor (R_w) is acceptable. Also, the weight ratio of $LiMnPO_4$(marked as LMP) to $Li_3V_2(PO_4)_3$ (marked as LVP) is 27.75:72.25, which is consistent with the molar ratio of 1:1, indicating the purity of rod-like $MnV_2O_6 \cdot 4H_2O$ precursor. It can be seen that the cell volume of LMP in the LMP·LVP/C composites decreases, compared with the pure orthorhombic LMP (space group Pnma, 25834-ICSD,), which may attribute to the V doping on the Mn sites because the ionic radius of V^{3+} (0.74Å) is smaller than that of Mn^{2+}(0.80Å). However, the cell volume of LVP in the LMP·LVP/C composites increases, compared with the monoclinic LVP(space group P21/n, 96962-ICSD), indicating that Mn is also doped into the LVP host lattice. The above results predict that the Mn^{2+} doping LVP and V^{3+}doping LMP coexist in the two-component composites for the utilization of $MnV_2O_6 \cdot 4H_2O$. As we know, this two-way behavior improved their electronic conductivity and electrochemical performance [18,24].

Based on the C-S analysis result, the carbon from glucose coating on the surface of LMP·LVP/C composite and existing in the form of carbon web between the particles add up to about 1.7wt.%. Oxalic acid, acted as reductant and decomposed into CO_2 and H_2O ultimately, was oven-contained in the composite. The SEM image of LMP·LVP/C synthesized at 700°C for 10 h is shown in Fig.4a.The particles in all samples have spheric-like morphology. In order to investigate the distribution and the carbon coating information in the LMP·LVP/C composites, TEM was employed in this paper. Fig.4b and c are the TEM images of the LMP·LVP/C synthesized at 700°C for 10 h. The primary particle size is about 200-400 nm and a conductive carbon network among the particles can also be observed in Fig.4b and c. HRTEM of region I was used to further study the microstructure of the as-prepared composites. Two regions of different framework are presented in Fig.4d. The lattice spacing of 0.23nm of the right region is corresponding to (012) of LMP phase and the lattice spacing of 0.26nm of the left region is corresponding to (113) of LVP

phase. Fig.4d indicates that the sample is a core-shell structure, which the external shell is amorphous carbon and the core of the sample are $LiMnPO_4$ unit cell and $Li_3V_2(PO_4)_3$ unit cell. The thickness of carbon shell is about 4.8nm.

Discussions

Fig.5a shows the initial charge-discharge curves of Li/$LiMnPO_4$·$Li_3V_2(PO_4)_3$/C cells at the rates of 0.05C, 0.1C, 3C and 10C. The excellent electrochemical performance of the composites may be due to the homogeneous distribution and the co-carbon source. With the proper addition of glucose and oxalic acid, the composites have a conductive network among the particles to improve the electronic conductivity of the material. So the structure of Li/$LiMnPO_4$·$Li_3V_2(PO_4)_3$/C was advantageous to the rate capability and the cyclic performances of the composite materials.

The cyclic voltammetry curves of LMP·LVP/C at a scan rate of 0.1 mVs^{-1} is presented in Fig.5b. It shows the redox peaks over the voltage range of 3-4.3V for the composite corresponding to the plateaus of charging and discharging curve. Three couple of redox peaks can be seen in the curves. The oxidation peaks of 3.64 and 3.73V are corresponded to the extraction of the first Li^+ in two steps: $Li_3V_2^{3+/3.5+}(PO_4)_3$ to $Li_{2.5}V_2^{3+/3.5+}(PO_4)_3$ and $Li_{2.5}V_2^{3.5+/4+}(PO_4)_3$ to $Li_2V_2^{3.5+/4+}(PO_4)_3$. The sharp oxidation peaks of 4.14V is corresponded to the extraction of the second Li^+: $Li_2V_2^{4+/5+}(PO_4)_3$ to $Li_1V_2^{4+/5+}(PO_4)_3$. The reduction peaks around 3.53V, 3.61V and 3.99V are corresponded to the insertion of the two Li^+. No characteristic peaks of LMP can be observed in the curves. This phenomenon is special and may be attributed to the reason that the peaks of LMP are covered by the peaks of LVP.

As seen in Fig.5c, the initial discharge capacity of LMP·LVP/C at the rate of 0.05C is about $136.5mAhg^{-1}$(The theoretic specific capacity (C_T) of LMP·LVP is calculated with the following equation: $C_T=(171X_1+133X_2)$ $(mAh\cdot g^{-1})$,where 171 and 133 are the theoretic capacities of LMP and LVP (<4.3V), respectively; X_1 and X_2 are the weight content of LMP and LVP, respectively. Based on our Rietveld refinement results(Tab.1 and Fig.3), the weight ratio of LVP is 72.25%, so the C_T for LMP·LVP/C synthesized in this paper is 143 $mAhg^{-1}$).The real capacity of the synthesized $LiMnPO_4$ is about $47mAhg^{-1}$, and about 96 $mAhg^{-1}$ for the $Li_3V_2(PO_4)_3$.

While, the initial discharge capacity of LMP·LVP/C at the rate of 0.1C, 3C and 10C can reach $126.2mAhg^{-1}$, $115.7mAhg^{-1}$ and $80.4mAhg^{-1}$. The discharge capacity is about $113.8mAhg^{-1}$

and 78.2 $mAhg^{-1}$after 30 cycles at the rate of 3C and 10C. The cell retains 98.35% and 97.3% of its initial discharge capacity, respectively. The composite material performs well at high rate. However, the discharge plateaus of LMP·LVP/C at different rates are fading obviously.

Conclusions

$LiMnPO_4 \cdot Li_3V_2(PO_4)_3$/C composite cathode material was synthesized from rod-like $MnV_2O_6 \cdot 4H_2O$ prepared by aqueous precipitation for the first time, following chemical reduction and lithiation with oxalic acid as the reducer and glucose as carbon sources. The $LiMnPO_4 \cdot Li_3V_2(PO_4)_3$/C compound synthesized at 700°C for 10h showed excellent electrochemical performance at high rate, and its discharge capacity is about 110 mAh g^{-1}, 104.4 mAh g^{-1}, 100.6 mAh g^{-1} and 80.4 mAh g^{-1} at the rate of 0.1C, 1C, 3C and 10C, respectively. The cell retains 97.1%, 97.0%, 92.1% and 97.3% of its initial discharge capacity after 20 cycles.

Acknowledgments

We gratefully acknowledge the financial support for this work of the National Natural Science Foundation of China (General Program) under grant number 51272290 and 51402365.

Notes and references

[1] A.K. Padhi, K.S. Nanjundaswamy, J.B. Goodenough, J. Electrochem. Soc., 1997, 144, 1188-1194.

[2] G. Yang, H.D. Liu, H.M. Ji, Z.Z. Chen, X.F. Jiang, J. Power Sources, 2010, 195, 5374-5378.

[3] K.T. Lee, W.H. Kan, L.F. Nazar, J. Am. Chem. Soc., 2009, 131, 6044-6045.

[4] H.D. Liu, G. Yang, X.F. Zhang, P. Gao, L. Wang, J.H. Fang, J. Pinto, X.F. Jiang, J. Mater. Chem., 2012, 22, 11039-11047.

[5] S. Patoux, C. Wurm, M. Morcrette, G. Rousse, C. Masquelier, J. Power Sources, 2003, 119, 278-284.

[6] S.C. Yin, H. Grondey, P. Strobel, M. Anne, L.F. Nazar, J. Am. Chem. Soc., 2003, 125, 10402-10411.

[7] H.D. Liu, P. Gao, J.H. Fang, G. Yang, Chem. Commun., 2011, 47, 9110-9112.

[8] C. Delacourt, L. Laffont, R. Bouchet, C. Wurm, J.-B. Leriche, M. Morcrette, J.-M. Tarascon, C. Masquelier, Journal of the Electrochemical Society, 2005, 152, A913.

[9] Y.Q. Qiao, J.P. Tu, X.L. Wang, C.D. Gu, Journal of Power Sources, 2012, 199, 287.

[10] G.X. Wang, S.L. Bewlay, K. Konstantinov, H.K. Liu, S.X. Dou, J.-H. Ahn, Electrochim. Acta, 2004, 50, 443.

[11] S.-Y. Chung, J.T. Bloking, Y.-M. Chiang, Nat. Mater., 2002, 1, 123.

[12] Y. Wen, L. Zeng, Z. Tong, L. Nong, J. Alloys Compd., 2006, 416, 206.

[13] X.J. Chen, G.S. Cao, X.B. Zhao, J.P. Tu, J. Alloys Compd., 2008, 463, 385.

[14] L. F. Fei, W. Lu, L. Sun, J.P Wang, J. B Wei, Helen L. W. Chan, Y. Wang, J. RSC. Adv., 2013, 3, 1297.

[15] L. Li, J. Liu, L. Chen, H. Y. Xu, J. Yang, Y. T. Qian, J. RSC. Adv., 2013, 3, 6847.

[16] H. Huang, S.C. Yin, L.F. Nazar, Electrochem. Soc., 2002, 149, 1184.

[17] T. Liu, J. J. Xu, B. B. Wu, Q. B. Xia, X. D. Wu, J. RSC Adv., 2013, 3, 13337.

[18] G. Yang, H. Ni, H. Liu, P. Gao, H. Ji, S. Roya, J. Pinto, X. Jiang, Journal of Power Sources, 2011, 196, 4747.

[19] F. Wang, J. Yang, Y. NuLi, J. -L. Wang, Electrochimica Acta, 2013,103, 96-102.

[20] L.-F. Qin, Y.-G. Xia, B Qiu, H.-L. Cao, Y.-Z. Liu, Z.-P. Liu, J. Power Sources, 2013, 239, 144-150.

[21] Brugger J, Berlepsch P, Meisser N, et al, The Canadian Mineralogist, 2003, 41, 1423-1431.

[22] Kim S S, Ikuta H, Wakihara M, Solid State Ionics, 2001, 139, 57-65.

[23] J. Brugger, P. Berlepsch, N. Meisser, The Canadian Mineralogist, 41(2003) 1423-1431.

[24] S.S. Kim, H. Ikuta, M. Wakihara, Solid State Ionics, 139 (2001) 57-65.